

Single-particle states in spherical Si/SiO₂ quantum dots

A.S. Moskalenko* and J. Berakdar

*Max-Planck-Institut für Mikrostrukturphysik, 06120 Halle & Institut für Physik,
Martin-Luther-Universität Halle-Wittenberg, Nanotechnikum-Weinberg,
Heinrich-Damerow-Str. 4, 06120 Halle, Germany*

A.A. Prokofiev and I.N. Yassievich

*Ioffe Physico-Technical Institute of RAS, 26 Polytechnicheskaya, 194021 St. Petersburg, Russia
(Dated: April 21, 2018)*

We calculate ground and excited electron and hole levels in spherical Si quantum dots inside SiO₂ in a multiband effective mass approximation. Luttinger Hamiltonian is used for holes and the strong anisotropy of the conduction electron effective mass in Si is taken into account. As boundary conditions for electron and hole wave functions we use continuity of the wave functions and the velocity density at the boundary of the quantum dots.

PACS numbers: 73.21.La, 73.22.Dj, 78.67.Hc, 78.60.-b

I. INTRODUCTION

The study of materials composed of Si nanocrystals dispersed in SiO₂ matrix is an issue of high importance for various optoelectronic applications^{1,2}. In particular, the knowledge of the energy spectrum of carriers confined in the nanocrystals and their wave functions is crucial for the understanding of electronic processes. Numerous theoretical works have been developed for the evaluations of the ground-state electron-hole pair energy of Si nanocrystals^{3,4,5,6,7,8}. On the other hand, the problem concerning the energy-level positions and the corresponding eigenfunctions of the excited carrier states is much less studied^{9,10}. However, shortly after the generation of an electron-hole pair in a nanocrystal a number of important non-equilibrium processes involving these "hot" carriers may take place¹¹ necessitating thus the knowledge of the excited states.

This current paper is devoted to the study of the ground and the excited electron and hole levels within the framework of a multiband effective mass approximation. The finite energy barriers at the Si/SiO₂ boundary are explicitly accounted for. For the description of the electron and hole states of the carriers confined in Si nanocrystals we utilize the envelope function approximation taking into account the elliptic symmetry of the bottom of the conduction band and the complex structure of the top of the valence band in Si. The finite energy barriers at the boundary between Si and SiO₂ are treated by employing the Bastard boundary conditions^{12,13}. This is mainly the difference of our method comparing to earlier calculations based on the effective mass approximation⁹ that failed to describe properly the optical properties of small nanocrystals. An advantage of our method in comparison with *ab-initio* methods based on the density functional theory^{5,8} is that without a considerable numerical effort we can calculate not only the ground state but also excited states of the confined carriers. Furthermore, our theory can be applied to a broad range of nanocrystal sizes. We are not limited to nanocrystals with a small

number of atoms. The other point is that the calculations of various excitation and de-excitation processes under participation of the confined carriers using the derived wave functions are transparent and allow for an insight into the underlying physics.

II. ELECTRON STATES

The conduction band of bulk Si has six equivalent minima in the first Brillouin zone at points $\pm\vec{k}_{0,z} = (0, 0, \pm 0.85)k_X$, $\pm\vec{k}_{0,y} = (0, \pm 0.85, 0)k_X$, and $\pm\vec{k}_{0,x} = (\pm 0.85, 0, 0)k_X$, where $k_X = 2\pi/a$ and $a = 0.543$ nm is the lattice constant of Si¹⁴. The minima are situated in the neighborhood of the six X -points (there are three non-equivalent X -points). The conduction band is doubly degenerate at each of the X -points, which is a consequence of the fact that Si lattice has two atoms in the elementary unit cell and the origin can be chosen at the center of any of them. Assuming the Bloch amplitudes not changing in the neighborhood of the X -point one can write the wave function of one of the six equivalent ground states of electrons in the nanocrystal as

$$\psi_\nu^e = \xi^e(\vec{r}) u_{c\nu} e^{i\vec{k}_{0,\nu}\vec{r}} \quad (\nu = \pm x, \pm y, \pm z), \quad (1)$$

where $u_{c\nu}$ is one of two Bloch amplitudes of bulk electron at X -point in the Brillouin zone, which corresponds to the lower conduction band at the $\vec{k}_{0,\nu}$ point. Note, that $u_{c\nu}$ yields zero overlap integral with the Bloch amplitudes of the top of the valence band¹⁵. The overlap integral of the Bloch amplitudes of the top of the valence band with the second Bloch amplitude $u_{s\nu} = u_{c\nu} e^{-i2\vec{k}_{X,\nu}\vec{r}}$ corresponding to the upper conduction band at $\vec{k}_{0,\nu}$ is not equal to zero. The envelope wave function ξ^e in Eq. (1)

inside the Si quantum dot satisfies the following equation:

$$\frac{\hbar^2}{2m_{\parallel}} \frac{\partial^2}{\partial z^2} \xi^e(x, y, z) + \frac{\hbar^2}{2m_{\perp}} \left(\frac{\partial^2}{\partial x^2} + \frac{\partial^2}{\partial y^2} \right) \xi^e(x, y, z) + E \xi^e(x, y, z) = 0, \quad (2)$$

where $m_{\parallel} = 0.916m_0$, $m_{\perp} = 0.19m_0$ with m_0 being the free electron mass. The rigorous formulation of the boundary conditions for the boundary between Si and SiO₂ in the framework of the envelope function method is not a trivial task and generally has to be investigated in comparison with experiment and numerical methods. The Bastard type boundary conditions imply that ξ and $\hat{v}\xi$ are continuous across the boundary, where $\hat{v} = \frac{1}{i\hbar}[\vec{r}, \hat{H}]$ is the velocity operator, ξ is the envelope wave function and \hat{H} is the corresponding Hamiltonian^{12,13}. Here we assume that the spectrum of electronic states outside the nanocrystal in SiO₂ is isotropic and determined by a single electron effective mass, which is equal to the free electron mass m_0 . Then outside the quantum dot we have

$$\frac{\hbar^2}{2m_0} \left(\frac{\partial^2}{\partial x^2} + \frac{\partial^2}{\partial y^2} + \frac{\partial^2}{\partial z^2} \right) \xi^e(x, y, z) + (E - U_e) \xi^e(x, y, z) = 0, \quad (3)$$

where U_e is the energy barrier for electrons. According to Ref. 10 we have $U_e = 3.2$ eV. The boundary conditions result in the following equations

$$\xi^e|_{r=R_{\text{nc}}^-} = \xi^e|_{r=R_{\text{nc}}^+}, \quad (4)$$

$$\left[\frac{1}{m_{\perp}} \frac{\rho}{R_{\text{nc}}} \frac{\partial \xi^e}{\partial \rho} + \frac{1}{m_{\parallel}} \frac{z}{R_{\text{nc}}} \frac{\partial \xi^e}{\partial z} \right]_{r=R_{\text{nc}}^-} = \frac{1}{m_0} \frac{\partial \xi^e}{\partial r} \Big|_{r=R_{\text{nc}}^+}, \quad (5)$$

which are most conveniently written in the cylindrical coordinate system (z, ρ, ϕ) .

Equations (2) and (3) with the boundary conditions (4) and (5) have been solved numerically after separating the trivial angular part $\frac{1}{\sqrt{2\pi}} \exp(im\phi)$ ($m = 0, \pm 1, \pm 2, \dots$) of the wave functions. We have got the electron energy levels and the corresponding envelope wave functions. The dependence of positions of the several lowest energy levels on the quantum dot diameter is depicted in Fig. 1. The dependence of the electron envelope wave functions on the distance from the center of the quantum dot is shown in Fig. 2 for $d = 2$ nm (such a small diameter is chosen for demonstration reasons in order to resolve better the tunnelling tails of the envelope wave functions). We have also compared the positions of the electron levels and their degeneracies with the existing data of Ref. 9 calculated by the empirical tight-binding method for quantum dots with diameter $d = 7.61$ nm. We have found that apart from small level splittings due to the valley-orbit interaction neglected in our model we get the same sequence of levels. The levels are, however, shifted towards

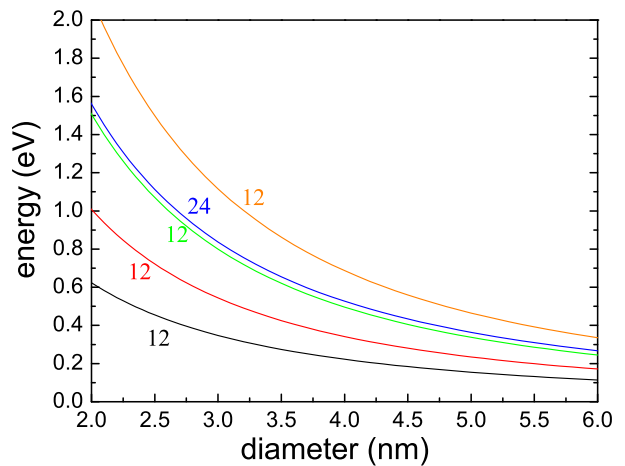


FIG. 1: (Color online) Dependence of positions of the electron energy levels above the bottom of the conduction band of bulk-Si on the quantum dot diameter. The numbers near the lines indicate the total degeneracy (including the spin degeneracy) of the corresponding levels.

the lower energies. The reason why we have smaller energies is that this tight-binding model used truncation of Si nanocrystals by H atoms. This procedure is known to give higher energies and greatly overestimate the optical band gap when compared with experiments on Si/SiO₂ nanocrystals and recent ab-initio TD-DFT calculations⁸ as well as with our model.

III. HOLE STATES

For description of the valence band structure in Si we use a generalization of the Luttinger Hamiltonian¹⁶ in the limit of a vanishing spin-orbit coupling, which is justified for Si, i.e. we write the Hamiltonian H in the form

$$\hat{H} = (A + 2B)\hat{p}^2 - 3B(\hat{p} \cdot \hat{J})^2, \quad (6)$$

where \hat{p} is the momentum operator and \hat{J} is the unitary angular momentum operator acting in the space of Bloch amplitudes. Furthermore, we introduced

$$A = -\frac{1}{4} \frac{m_h + m_l}{m_h m_l}, \quad B = -\frac{1}{4} \frac{m_h - m_l}{m_h m_l}, \quad (7)$$

$$m_h = \frac{m_0}{\gamma_1 - 2\gamma}, \quad m_l = \frac{m_0}{\gamma_1 + 2\gamma}, \quad \gamma = \frac{1}{5}(3\gamma_3 + 2\gamma_2). \quad (8)$$

Values of the constants γ_1 , γ_2 , and γ_3 for Si are 4.22, 0.53, and 1.38, respectively¹⁴. The basis of the Bloch amplitudes space can be chosen in the form of spherical components¹⁷ $u_0 = Z$, $u_{\pm} = \mp \sqrt{1/2}(X \pm iY)$ of the corresponding functions $X = yz$, $Y = xz$, and $Z = xy$, of the representation $\Gamma_{25'}$ ^{12,15}.

In the bulk Si this model leads to two types of states corresponding to a doubly degenerate (in absence of spin-dependent interactions) heavy hole band having mass

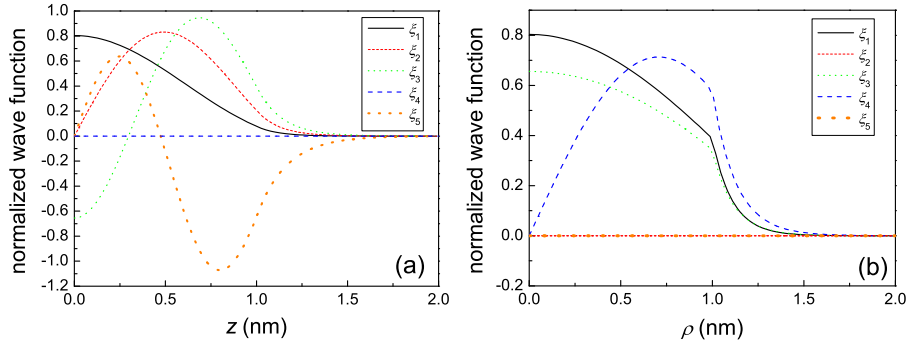


FIG. 2: (Color online) Electron wave functions in dependence on the cylindrical coordinates z (a) and ρ (b) for five lowest electron levels of a quantum dot with diameter of 2 nm. The wave function ξ_4^z of the fourth level with magnetic number $m = \pm 1$ has also an angular dependence $e^{im\phi}$.

m_h and a non-degenerate light hole band having mass $2m_h m_l / (3m_h - m_l)$. The quantum confinement gives rise to mixing of the states. Eigenfunctions of the Hamiltonian (6) can be found as eigenfunctions ψ_{FM} of the square \hat{F}^2 of the full angular momentum operator $\hat{F} = \hat{L} + \hat{J}$ ($\hat{L} = -i\vec{r} \times \partial_{\vec{r}}$) and its projection \hat{F}_z onto the axis z ¹⁸. Eigenvalues of \hat{F}^2 and \hat{F}_z are $F(F+1)$ and M , respectively, where $F = 0, 1, 2, \dots$ and M can be any integer number having absolute value not larger than F . For a spherical quantum dot there are three types of states, namely

$$\psi_{FM}^{F-1, F+1}(r, \theta, \phi) = R_F^{F-1}(r) \mathbf{Y}_{FM}^{F-1}(\theta, \phi) + R_F^{F+1}(r) \mathbf{Y}_{FM}^{F+1}(\theta, \phi), \quad (9)$$

$$\psi_{FM}^F(r, \theta, \phi) = R_F^F(r) \mathbf{Y}_{FM}^F(\theta, \phi), \quad (10)$$

$$\psi_{00}^1(r, \theta, \phi) = R_0^1(r) \mathbf{Y}_{00}^1(\theta, \phi), \quad (11)$$

where $R_F^{F-1}(r)$, $R_F^{F+1}(r)$, and $R_F^F(r)$ are the radial parts of the envelope wave functions. Furthermore,

$$\mathbf{Y}_{FM}^L(\theta, \phi) = \sum_{m_1, m_2} C_{Lm_1 m_2}^{FM} Y_{Lm_1}(\theta, \phi) u_{m_2} \quad (12)$$

are the vector spherical harmonics that can be expressed in terms of the usual spherical harmonics $Y_{nm}(\theta, \phi)$ and the Clebsch-Gordan coefficients $C_{j_1 m_1 j_2 m_2}^{j m}$ ¹⁹. For the first two types of functions (9) and (10) only solutions with $F \geq 1$ are possible. We will see that the functions (9) are of a mixed type, whereas the functions (10) and (11) are of a heavy and light hole type, respectively.

For a formulation of the boundary conditions for the hole states we take into account that the main contribution to the valence band states in SiO₂ is given by p -orbitals²⁰ and for description of hole states outside the Si nanocrystal we can use the same form of the Luttinger Hamiltonian (6). It is known that the hole masses at the valence band maximum in SiO₂ are pretty large²⁰. For simplicity we choose them to be equal to $m_v = 5m_0$. Then the corresponding values of the coefficients A_o and B_o of the Luttinger Hamiltonian (6) are $A_o = -\frac{1}{2m_v}$ and $B_o = 0$. In such a case we can formulate appropriate Bastard type boundary conditions.

Inserting the functions $\psi_{FM}^{F-1, F+1}$ given by Eq. (9) into the Schrödinger equation with the Hamiltonian (6) we get the following equation system (see also Ref. 18) for the radial functions $R_F^{F-1}(r)$, $R_F^{F+1}(r)$ inside the nanocrystal ($r < R_{nc}$):

$$\left(1 + \frac{F-1}{2F+1}\mu\right) \left[\frac{d^2}{dr^2} + \frac{2}{r} \frac{d}{dr} - \frac{(F-1)F}{r^2}\right] R_F^{F-1}(r) - \frac{3\sqrt{F(F+1)}}{2F+1}\mu \left[\frac{d^2}{dr^2} + \frac{2F+3}{r} \frac{d}{dr} + \frac{F(F+2)}{r^2}\right] R_F^{F+1}(r) = -\frac{E}{A\hbar^2} R_F^{F-1}(r), \quad (13)$$

$$-\frac{3\sqrt{F(F+1)}}{2F+1}\mu \left[\frac{d^2}{dr^2} - \frac{2F-1}{r} \frac{d}{dr} + \frac{(F-1)(F+1)}{r^2}\right] R_F^{F-1}(r) + \left(1 + \frac{F+2}{2F+1}\mu\right) \left[\frac{d^2}{dr^2} + \frac{2}{r} \frac{d}{dr} - \frac{(F+1)(F+2)}{r^2}\right] R_F^{F+1}(r) = -\frac{E}{A\hbar^2} R_F^{F+1}(r), \quad (14)$$

where E denote the hole energy and $\mu = B/A$. The general solution of the equation system of Eqs. (13) and (14), which does not diverge at $r = 0$, is found as

$$R_F^{F-1}(r) = \mathcal{C}j_{F-1}(\lambda r/R_{\text{nc}}) + \mathcal{D}j_{F-1}(\lambda\beta r/R_{\text{nc}}), \quad (15)$$

$$R_F^{F+1}(r) = -\sqrt{\frac{F}{F+1}}\mathcal{C}j_{F+1}(\lambda r/R_{\text{nc}}) + \sqrt{\frac{F+1}{F}}\mathcal{D}j_{F+1}(\lambda\beta r/R_{\text{nc}}), \quad (16)$$

where \mathcal{C} , \mathcal{D} are coefficients to be found from the boundary and normalization conditions, $j_l(z)$ are the spherical Bessel functions of the first kind²¹, and

$$\beta = \sqrt{\frac{1-\mu}{1+2\mu}}. \quad (17)$$

The energy E , which is negative, is connected with the positive variable λ via

$$E = \frac{A\hbar^2}{R_{\text{nc}}^2}(1-\mu)\lambda^2 = -\frac{\hbar^2}{2m_h R_{\text{nc}}^2}\lambda^2. \quad (18)$$

Outside of the nanocrystal ($r > R_{\text{nc}}$) the radial parts of the functions $\psi_{FM}^{F-1, F+1}$ satisfy the following equations

$$A_o\hbar^2 \left[\frac{d^2}{dr^2} + \frac{2}{r} \frac{d}{dr} - \frac{(F-1)F}{r^2} \right] R_F^{F-1}(r) = -(E + U_h)R_F^{F-1}(r), \quad (19)$$

$$A_o\hbar^2 \left[\frac{d^2}{dr^2} + \frac{2}{r} \frac{d}{dr} - \frac{(F+1)(F+2)}{r^2} \right] R_F^{F+1}(r) = -(E + U_h)R_F^{F+1}(r), \quad (20)$$

where U_h is the energy barrier for holes at the Si/SiO₂ boundary. According to Ref. 10 we have $U_h = 4.3$ eV. The general solution of the equation system of Eqs. (19) and (20), which converges to zero for large distances from the nanocrystal is found as

$$R_F^{F-1}(r) = (\mathcal{C}_o + \mathcal{D}_o)k_{F-1}(\kappa r/R_{\text{nc}}), \quad (21)$$

$$R_F^{F+1}(r) = \left(-\sqrt{\frac{F}{F+1}}\mathcal{C}_o + \sqrt{\frac{F+1}{F}}\mathcal{D}_o \right) k_{F+1}(\kappa r/R_{\text{nc}}), \quad (22)$$

where

$$\kappa = \frac{\sqrt{2m_v(E + U_h)} R_{\text{nc}}}{\hbar}, \quad (23)$$

\mathcal{C}_o , \mathcal{D}_o are again coefficients to be found from the boundary and normalization conditions, and $k_l(z)$ are the modified spherical Bessel functions of the third kind²¹. The boundary conditions lead to the following equations for the radial functions:

$$R_F^{F-1}(r) \Big|_{r=R_{\text{nc}}^-} = R_F^{F-1}(r) \Big|_{r=R_{\text{nc}}^+}, \quad (24)$$

$$R_F^{F+1}(r) \Big|_{r=R_{\text{nc}}^-} = R_F^{F+1}(r) \Big|_{r=R_{\text{nc}}^+}, \quad (25)$$

$$\left[\left(\left(A + \frac{F-1}{2F+1} B \right) \frac{d}{dr} + \frac{3}{2} \frac{F-1}{2F+1} \frac{B}{r} \right) R_F^{F-1}(r) - \frac{3\sqrt{F(F+1)}}{2F+1} B \left(\frac{d}{dr} + \frac{F+2}{r} \right) R_F^{F+1}(r) \right]_{r=R_{\text{nc}}^-} = A_o \frac{d}{dr} R_F^{F-1}(r) \Big|_{r=R_{\text{nc}}^+}, \quad (26)$$

$$\left[-\frac{3\sqrt{F(F+1)}}{2F+1} B \left(\frac{d}{dr} - \frac{F-1}{r} \right) R_F^{F-1}(r) + \left(\left(A + \frac{F+2}{2F+1} B \right) \frac{d}{dr} + \frac{3}{2} \frac{F+2}{2F+1} \frac{B}{r} \right) R_F^{F+1}(r) \right]_{r=R_{\text{nc}}^-} = A_o \frac{d}{dr} R_F^{F+1}(r) \Big|_{r=R_{\text{nc}}^+}. \quad (27)$$

Using the functions (15), (16) and (21), (22) in Eqs. (24)-(27) leads to a solvability condition determining the energy eigenvalues for states $\psi_{FM}^{F-1, F+1}$. We have derived this condition (see Appendix). From it we have found numerically the energy eigenvalues in dependence on the nanocrystal radius R_{nc} . The corresponding coefficients \mathcal{C} , \mathcal{D} , \mathcal{C}_o , and \mathcal{D}_o , assuring the normalization condition, have been also derived numerically.

For the radial function $R_F^F(r)$ of the states ψ_{FM}^F we get the following equation inside the Si quantum dot

$$(1-\mu) \left[\frac{d^2}{dr^2} + \frac{2}{r} \frac{d}{dr} - \frac{F(F+1)}{r^2} \right] R_F^F(r) = -\frac{E}{A\hbar^2} R_F^F(r). \quad (28)$$

One can easily see that it is the same equation as for the radial part of wave function of a particle having a simple

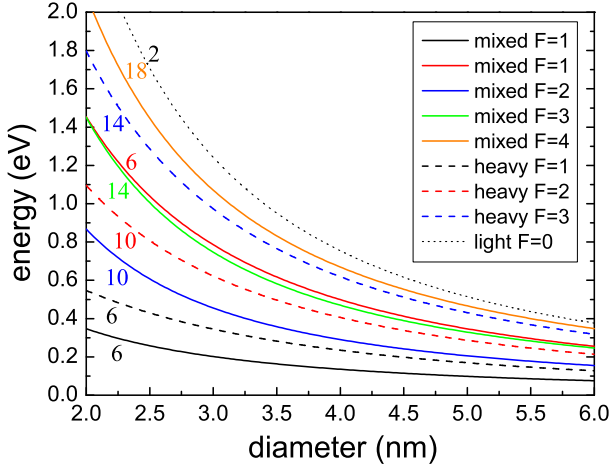


FIG. 3: (Color online) Dependence of the positions of the hole energy levels below the top of the valence band of bulk-Si on the quantum dot diameter. The numbers near the lines indicate the total degeneracy (including the spin degeneracy) of the corresponding levels. Types of the levels and values of the total angular momentum F are also shown.

parabolic band with the heavy hole mass and angular momentum F . For the radial function $R_0^1(r)$ of the states ψ_{00}^1 we get

$$(1 + 2\mu) \left[\frac{d^2}{dr^2} + \frac{2}{r} \frac{d}{dr} - \frac{2}{r^2} \right] R_0^1(r) = -\frac{E}{A\hbar^2} R_0^1(r). \quad (29)$$

This equation is then the same as for a simple particle having the light hole mass and angular momentum 1. Solving equations (28) and (29) we find

$$R_F^F(r) = \mathcal{C}' j_F(\lambda r/R_{nc}), \quad (30)$$

$$R_0^1(r) = \mathcal{C}'' j_1(\lambda \beta r/R_{nc}), \quad (31)$$

for $r < R_{nc}$, where \mathcal{C}' and \mathcal{C}'' are the corresponding normalization coefficients. Outside the nanocrystal $R_F^F(r)$ satisfies the equation

$$A_o \hbar^2 \left[\frac{d^2}{dr^2} + \frac{2}{r} \frac{d}{dr} - \frac{F(F+1)}{r^2} \right] R_F^F(r) = -(E+U_h) R_F^F(r) \quad (32)$$

and $R_0^1(r)$ satisfies the equation

$$A_o \hbar^2 \left[\frac{d^2}{dr^2} + \frac{2}{r} \frac{d}{dr} - \frac{2}{r^2} \right] R_0^1(r) = -(E+U_h) R_0^1(r). \quad (33)$$

Solutions having an appropriate behavior at infinity are

$$R_F^F(r) = \mathcal{C}'_o k_F(\kappa r/R_{nc}), \quad (34)$$

$$R_0^1(r) = \mathcal{C}''_o k_1(\kappa r/R_{nc}). \quad (35)$$

The boundary conditions in this case are found as

$$R_F^F(r) \Big|_{r=R_{nc}^-} = R_F^F(r) \Big|_{r=R_{nc}^+}, \quad (36)$$

$$\left[(A-B) \frac{d}{dr} - \frac{3B}{2r} \right] R_F^F(r) \Big|_{r=R_{nc}^-} = A_o \frac{d}{dr} R_F^F(r) \Big|_{r=R_{nc}^+}, \quad (37)$$

for $R_F^F(r)$ functions, and

$$R_0^1(r) \Big|_{r=R_{nc}^-} = R_0^1(r) \Big|_{r=R_{nc}^+}, \quad (38)$$

$$\left[(A+2B) \frac{d}{dr} + \frac{3B}{r} \right] R_0^1(r) \Big|_{r=R_{nc}^-} = A_o \frac{d}{dr} R_0^1(r) \Big|_{r=R_{nc}^+}, \quad (39)$$

for $R_0^1(r)$ functions. Using the form of the radial wave functions given by Eqs. (30),(34) [Eqs. (31),(35)] in Eqs. (36),(37) [Eqs. (38),(39)] we get the equation determining the energy levels of states ψ_{FM}^F [ψ_{00}^1] (see Appendix). Solving this equation numerically we have found energy level positions of holes of the heavy and light hole types.

The dependence of positions of the hole energy levels on the nanocrystal radius, their types and degeneracies are presented in Fig. 3 for several lowest hole levels. One can see that the hole level structure is more dense in comparison with the electron level structure. This can lead to important differences in behavior of "hot" electrons and holes²².

IV. COULOMB SHIFT

The Coulomb interaction leads to a decrease of the recombination energy of an electron-hole pair²³. This interaction should be considered taking into account the "image charge" effects appearing because of the dielectric constant difference at the quantum dot boundary. On the other side the dielectric constant mismatch leads to interaction of a charged particle with its own image. Resulting polarization self-energy correction increases single-particle energies of electrons and holes (counted upwards from the bottom of the bulk conduction band and downwards from the top of the valence band, respectively). If the dielectric constant changes discontinuously at the quantum dot boundary the polarization self-interaction diverges there. This is not an immediate problem for models of quantum dots assuming infinite energy barriers for electrons and holes at the quantum dot boundary because particle wave functions vanish there and the self-energy correction induced by the self-interaction remains finite^{24,25,26}. However, as a consequence of finite energy barriers particle wave functions are finite at the quantum dot boundary (see Fig. 2) and self-energy corrections become infinite.

In order to remove these unphysical divergences one has to take into account that the position-dependent dielectric constant should change smoothly between the values corresponding to the quantum dot core and the surrounding material on the scale of the interatomic distance. This can be done in a simple and intuitive way by "regularizing" directly the self-interaction^{27,28}. A

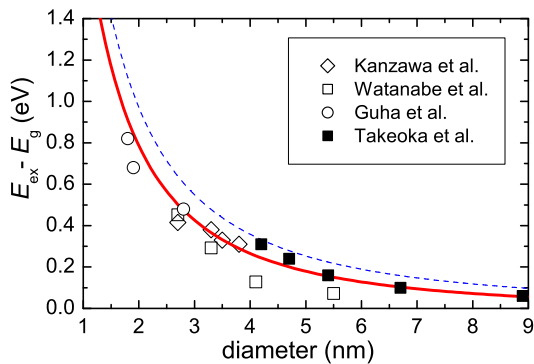


FIG. 4: (Color online) Dependence of the ground-state electron-hole recombination energy as a function of diameter of nanocrystal (solid line). Dashed line shows the same energy without taking into account the exciton shift. For comparison, the experimental data obtained from photoluminescence spectra^{32,33,34,35} measured for Si nanocrystals inside SiO₂ are presented.

more physical and controllable, however more demanding way is to solve the problem with the smooth position-dependent dielectric constant²⁹. Calculations of Ref. 29 show that the total correction to the electron-hole pair energy introduced by the Coulomb and "image charge" interactions depends strongly on the width of the transition region between two values of the dielectric constant. For reasonable values of the transition region width around the interatomic distance the corrections introduced by the electron-hole Coulomb interaction and the polarization self-energy corrections cancel each other to high extent. Therefore, the overall Coulomb correction to the energy of the electron-hole pair is small and electron-hole recombination energy is pretty accurately given by the sum of the band gap with the electron and hole single-particle quantization energies. This conclusion is also supported by GW calculations for small hydrogen-terminated silicon nanocrystals³⁰.

An estimate (rather an upper limit estimate²⁹) of the overall Coulomb shift V_C can be deduced using single-particle wave functions corresponding to infinitely high energy barriers. We have calculated V_C under these assumptions treating the Coulomb correction as a perturbation to the single-particle Hamiltonian^{26,31}. The result for the ground-state electron and hole can be given then in a simple form: $V_C = -1.54e^2/(\kappa_{\text{Si}}R_{\text{nc}})$, where κ_{Si} is the dielectric constant of Si and it was taken into account that the surrounding material has an approximately three times smaller dielectric constant than Si (one should notice that Ref. 26 gives a different numerical constant computed incorrectly by us). The excitonic shift calculated in the same way for higher states of electrons and hole is on the same order and smaller.

In Fig. 4 the dependence of the exciton energy as a function of diameter of the nanocrystal is presented for the ground state. This dependence is also shown when the excitonic energy shift is accounted for. The theory is

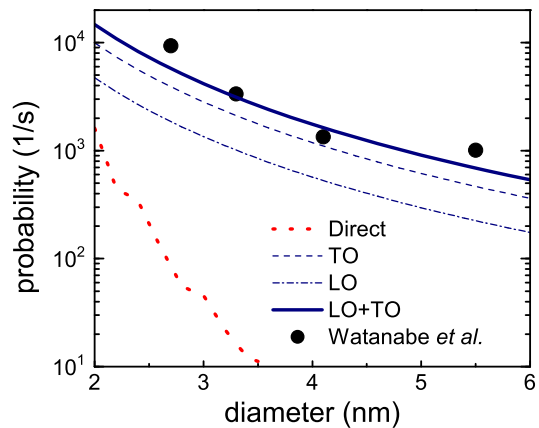


FIG. 5: (Color online) Probabilities $P_{r,gr}$ of radiative transitions between the ground electron and hole states: assisted by emission of a TO-phonon (dashed line), an LO-phonon (dash-dot line) and their sum (thick solid line) as well as probability of direct (zero-phonon) transition (dot line), as functions of nanocrystal diameter. Experimental points³⁵ are shown as well.

compared with the experimental data obtained from the photoluminescence spectra^{32,33,34,35}.

V. RADIATIVE RECOMBINATION

We have produced calculation of the probabilities P_r of radiative recombination assisted by emission of an optical transverse phonon (with energy 57.5 meV) as well as longitudinal one (55.3 meV). These channels of radiative transitions dominate in bulk Si. The details of the calculation will be published in a separate paper. The results of calculations for the ground exciton state ($P_{r,gr}$) are presented in Fig. 5. The probabilities of radiative transitions involving excited states P_r have similar dependences on nanocrystal size being of the same order of magnitude (e.g. for transition from the second electron state to the first hole state $P_r \approx 0.8P_{r,gr}$). In Fig. 5 the result of calculations of direct (zero-phonon) radiative transition for the ground exciton state is presented as well. Such a transition becomes possible for confined carriers but one can see that the oscillator strength is noticeably less for the dots with diameter larger than 2 nm. This is a well-known experimental fact³⁶. One should notice that the shown probability of the direct radiative transition has been calculated as an average value over the nanocrystal size distribution in order to achieve the acceptable convergence of the numerical integration and to avoid strong oscillations of the result^{37,38}. One can see from Fig. 5 that our results reproduce the experimental data on radiative lifetimes in Si/SiO₂ nanocrystals³⁵ very well. As far as radiative transitions most probably take place together with a phonon emission the exciton band gap derived from the photoluminescence spectra should generally be lower than the calculated one by the amount

of the phonon energy (cf. Fig. 4).

VI. CONCLUSION

We have calculated the wave functions and the energy levels of confined carriers in Si quantum dots inside a SiO₂ matrix as functions of the dot diameter. It has been shown that for small quantum dots ($d \lesssim 2.5$ nm) the energy spacing between neighboring electron and hole levels is of the order of hundreds of meV, and for electrons they are larger than for holes. Such energy spacings are also larger than the energy level splittings due to different mechanisms⁹, which are not accounted for in this paper. Therefore, the single-phonon relaxation between the levels becomes impossible and the time of relaxation of "hot" carriers to the ground state should increase. The calculated recombination energies of an electron-hole pair in the ground state and the probabilities of radiative interband transitions between the ground electron and hole levels are in good agreement with ex-

perimental data. Comparison of the electron and hole levels calculated by our method and by state-of-the-art computational methods⁸ could lead in the future to a more rigorous formulation of the boundary conditions in the framework of the multiband effective mass approximation. This would allow to produce rather quantitative calculations of processes involving electrons and holes in Si nanocrystals with a reasonable computational effort.

Acknowledgement.- We thank Prof. E.L. Ivchenko and Prof. V.I. Perel for useful discussions. On the Russian side, this work was partly financially supported by RFBR, NWO, INTAS, RAS. One of the authors (A. A. P.) was also supported by the Dynasty Foundation.

APPENDIX: EQUATIONS FOR QUANTIZATION ENERGIES OF HOLES

Equations determining the energy quantization levels for holes of mixed, heavy and light holes are

$$\begin{aligned}
& \left[\nu\kappa \left(\frac{F-1}{2F-1} \frac{k_{F-2}(\kappa)}{k_{F-1}(\kappa)} + \frac{F}{2F-1} \frac{k_F(\kappa)}{k_{F-1}(\kappa)} \right) j_{F-1}(\lambda) + \left(1 + \frac{F-1}{2F+1} \mu \right) \lambda \left(\frac{F-1}{2F-1} j_{F-2}(\lambda) - \frac{F}{2F-1} j_F(\lambda) \right) \right. \\
& \quad \left. + \mu \left(\frac{3}{2} \frac{F-1}{2F+1} j_{F-1}(\lambda) + \frac{3F(F+2)}{2F+1} j_{F+1}(\lambda) \right) + \frac{3F}{2F+1} \mu \lambda \left(\frac{F+1}{2F+3} j_F(\lambda) - \frac{F+2}{2F+3} j_{F+2}(\lambda) \right) \right] \\
& \times \left[\frac{F+1}{F} \nu\kappa \left(\frac{F+1}{2F+3} \frac{k_F(\kappa)}{k_{F+1}(\kappa)} + \frac{F+2}{2F+3} \frac{k_{F+2}(\kappa)}{k_{F+1}(\kappa)} \right) j_{F+1}(\lambda\beta) - 3 \frac{F+1}{2F+1} \mu \lambda \beta \left(\frac{F-1}{2F-1} j_{F-2}(\lambda\beta) - \frac{F}{2F-1} j_F(\lambda\beta) \right) \right. \\
& \quad \left. + \mu \left(\frac{3(F^2-1)}{2F+1} j_{F-1}(\lambda\beta) + \frac{3}{2} \frac{(F+1)(F+2)}{F(2F+1)} j_{F+1}(\lambda\beta) \right) \right. \\
& \quad \left. + \frac{F+1}{F} \left(1 + \frac{F+2}{2F+1} \mu \right) \lambda \beta \left(\frac{F+1}{2F+3} j_F(\lambda\beta) - \frac{F+2}{2F+3} j_{F+2}(\lambda\beta) \right) \right] = \\
& \left[\nu\kappa \left(\frac{F-1}{2F-1} \frac{k_{F-2}(\kappa)}{k_{F-1}(\kappa)} + \frac{F}{2F-1} \frac{k_F(\kappa)}{k_{F-1}(\kappa)} \right) j_{F-1}(\lambda\beta) + \left(1 + \frac{F-1}{2F+1} \mu \right) \lambda \beta \left(\frac{F-1}{2F-1} j_{F-2}(\lambda\beta) - \frac{F}{2F-1} j_F(\lambda\beta) \right) \right. \\
& \quad \left. + \mu \left(\frac{3}{2} \frac{F-1}{2F+1} j_{F-1}(\lambda\beta) - \frac{3(F+1)(F+2)}{2F+1} j_{F+1}(\lambda\beta) \right) - \frac{3(F+1)}{2F+1} \mu \lambda \beta \left(\frac{F+1}{2F+3} j_F(\lambda\beta) - \frac{F+2}{2F+3} j_{F+2}(\lambda\beta) \right) \right] \\
& \times \left[-\nu\kappa \left(\frac{F+1}{2F+3} \frac{k_F(\kappa)}{k_{F+1}(\kappa)} + \frac{F+2}{2F+3} \frac{k_{F+2}(\kappa)}{k_{F+1}(\kappa)} \right) j_{F+1}(\lambda) - \frac{3(F+1)}{2F+1} \mu \lambda \left(\frac{F-1}{2F-1} j_{F-2}(\lambda) - \frac{F}{2F-1} j_F(\lambda) \right) \right. \\
& \quad \left. + \mu \left(\frac{3(F^2-1)}{2F+1} j_{F-1}(\lambda) - \frac{3}{2} \frac{F+2}{2F+1} j_{F+1}(\lambda) \right) - \left(1 + \frac{F+2}{2F+1} \mu \right) \lambda \left(\frac{F+1}{2F+3} j_F(\lambda) - \frac{F+2}{2F+3} j_{F+2}(\lambda) \right) \right], \tag{A1}
\end{aligned}$$

$$(1-\mu)\lambda \left[\frac{F}{2F+1} j_{F-1}(\lambda) - \frac{F+1}{2F+1} j_{F+1}(\lambda) \right] - \frac{3}{2} \mu j_F(\lambda) + \nu\kappa j_F(\lambda) \left[\frac{F}{2F+1} \frac{k_{F-1}(\kappa)}{k_F(\kappa)} + \frac{F+1}{2F+1} \frac{k_{F+1}(\kappa)}{k_F(\kappa)} \right] = 0, \tag{A2}$$

$$(1+2\mu)\lambda\beta [j_0(\lambda\beta) - 2j_2(\lambda\beta)] k_1(\kappa) + 9\mu j_1(\lambda\beta) k_1(\kappa) + \eta\kappa j_1(\lambda\beta) [k_0(\kappa) + 2k_2(\kappa)] = 0, \tag{A3}$$

respectively. Here $\mu = B/A$, $\nu = A_o/A$, β is defined by Eq. (17), λ and κ are functions of the hole energy E

determined by Eq. (18) and Eq. (23), respectively.

-
- * Also at Ioffe Physico-Technical Institute of RAS, 26 Polytechnicheskaya, 194021 St. Petersburg, Russia; Electronic address: moskalen@mpi-halle.de
- ¹ L. Pavesi, L. Dal Negro, C. Mazzoleni, G. Franzo, and F. Priolo, *Nature* (London) **440**, 408 (2000).
 - ² A. Polman, *Nat. Mater.* **1**, 10 (2002).
 - ³ J.P. Proot, C. Delerue, and G. Allan, *Appl. Phys. Lett.* **61**, 1948 (1992).
 - ⁴ E. Martin, C. Delerue, G. Allan, and M. Lannoo, *Phys. Rev. B* **50**, 18258 (1994).
 - ⁵ B. Delley and E.F. Steigmeier, *Phys. Rev. B* **47**, 1397 (1993).
 - ⁶ L.-W. Wang and A. Zunger, *J. Chem. Phys.* **100**, 2394 (1994).
 - ⁷ M.V. Wolkin, J. Jorne, P.M. Fauchet, G. Allan, and C. Delerue, *Phys. Rev. Lett.* **82**, 197 (1999).
 - ⁸ C.S. Garoufalis and A.D. Zdetsis, *Phys. Chem. Chem. Phys.* **8**, 808 (2006).
 - ⁹ Y.M. Niquet, C. Delerue, G. Allan, and M. Lannoo, *Phys. Rev. B* **62**, 5109 (2000).
 - ¹⁰ V.A. Burdov, *JETP* **94**, 411 (2002).
 - ¹¹ I. Izeddin, A.S. Moskalenko, I.N. Yassievich, M. Fujii, and T. Gregorkiewicz, *Phys. Rev. Lett.* **97**, 207401 (2006).
 - ¹² P. Yu and M. Cardona, *Fundamentals of semiconductors. Physics and Material Properties* (Third Edition) (Springer, Berlin, 2001).
 - ¹³ E.L. Ivchenko and G.E. Pikus, *Superlattices and Other Heterostructures* (Springer, Berlin, 1997).
 - ¹⁴ A. Dargys, J. Kundrotas, *Handbook on Physical Properties of Ge, Si, GaAs and InP* (Science and Encyclopedia Publishers, Vilnius, 1994).
 - ¹⁵ M. Cardona and F.H. Pollak, *Phys. Rev.* **142**, 530 (1966).
 - ¹⁶ V. N. Abakumov, V. I. Perel, and I. N. Yassievich, *Nonradiative Recombination in Semiconductors*, in V. M. Agranovich and A. A. Maradudin (Eds.), *Modern Problems in Condensed Matter Sciences*, Vol. 33 (Elsevier, Amsterdam, 1991).
 - ¹⁷ A.R. Edmonds, *Angular momentum in quantum mechanics* (University Press, Princeton, 1957).
 - ¹⁸ A. Baldereschi and N. O. Lipari, *Phys. Rev. B* **8**, 2697 (1973).
 - ¹⁹ D.A. Varshalovich, A.N. Moskalev, and V.K. Khersonskii, *Quantum Theory of Angular Momentum* (World Scientific, Singapore, 1988).
 - ²⁰ J.R. Chelikowsky and M. Schlüter, *Phys. Rev. B* **15**, 4020 (1977).
 - ²¹ *Handbook of Mathematical Functions*, edited by M. Abramowitz and I.A. Stegun (Dover, New York, 1972).
 - ²² E. Hendry, M. Koeberg, F. Wang, H. Zhang, C. de Mello Donega, D. Vanmaekelbergh, and M. Bonn, *Phys. Rev. Lett.* **96**, 057408 (2006).
 - ²³ A.I.L. Efros and A.L. Efros, *Fiz. Tekh. Poluprovodn.* **16**, 1209 (1982) [*Sov. Phys. Semicond.* **16**, 772 (1982)].
 - ²⁴ L.E. Brus, *J. Chem. Phys.* **80**, 4403 (1984).
 - ²⁵ M. Lannoo, C. Delerue, and G. Allan, *Phys. Rev. Lett.* **74**, 3415 (1995).
 - ²⁶ A.S. Moskalenko, I.N. Yassievich, *Phys. Sol. State* **46**, 1508 (2004).
 - ²⁷ L. Banyai, P. Gilliot, Y.Z. Hu, and S.W. Koch, *Phys. Rev. B* **45**, 14136 (1992).
 - ²⁸ A. Franceschetti and A. Zunger, *Physical Review B* **62**, 2614 (2000).
 - ²⁹ P.G. Bolcatto and C.R. Proetto, *J. Phys.: Condens. Matter* **13**, 319 (2001).
 - ³⁰ C. Delerue, M. Lannoo, and G. Allan, *Phys. Rev. Lett.* **84**, 2457 (2000).
 - ³¹ I.N. Yassievich, A.S. Moskalenko, and A.A. Prokofiev, *Mater. Sci. Eng. C* (in press).
 - ³² Y. Kanzawa, T. Kageyama, S. Takeda, M. Fujii, S. Hayashi, and K. Yamamoto, *Solid State Commun.* **102**, 533 (1997).
 - ³³ S. Guha, B. Qadri, R.G. Musket, M.A. Wall, and T. Shimizu-Iwayama, *J. Appl. Phys.* **88**, 3954 (2000).
 - ³⁴ S. Takeoka, M. Fujii, and S. Hayashi, *Phys. Rev. B* **62**, 16820 (2000).
 - ³⁵ K. Watanabe, M. Fujii, and S. Hayashi, *J. Appl. Phys.* **90**, 4761 (2001).
 - ³⁶ D. Kovalev, H. Heckler, M. Ben-Chorin, G. Polisski, M. Schwartzkopff, and F. Koch, *Phys. Rev. Lett.* **81**, 2803 (1998).
 - ³⁷ M.S. Hybertsen, *Phys. Rev. Lett.* **72**, 1514 (1994).
 - ³⁸ C. Delerue, G. Allan, and M. Lannoo, *Phys. Rev. B* **64**, 193402 (2001).